Separable-Potential Fits to Nucleon-Nucleon Scattering Data*

THOMAS R. MONGAN
Lawrence Radiation Laboratory, University of California, Berkeley, California 94720
(Received 10 June 1968)

The Arndt-MacGregor (Livermore) nucleon-nucleon phase shifts and mixing parameters for partial waves through $J=4$ are fitted in the energy range 0–400 MeV by separable potentials. We have demanded that the partial-wave scattering amplitudes resulting from our potentials have singularities *only* for real negative values of the complex energy variable, in addition to the usual right-hand unitarity cut guaranteed by the Lippman-Schwinger formalism. We have also demanded that the appropriate partial-wave amplitudes contain the deuteron pole and the singlet antibound-state pole at the correct energies. The use of these fits in probing the off-energy-shell behavior of scattering amplitudes is discussed.

I. INTRODUCTION

THE main reason for the use of nonlocal separable potentials to describe the interaction between particles is their extreme convenience and simplicity. Also, separable potentials provide a simple extension of the two-body scattering amplitude off the energy shell, because the separable-potential form factors determine the off-energy-shell behavior of the scattering amplitude in a relatively transparent manner.

A representation of the off-energy-shell two-body partial-wave transition amplitude for a particular process should satisfy five general nondynamical requirements.[1] In the case of nucleon-nucleon scattering, we shall show that separable-potential forms may be chosen which lead to scattering amplitudes that fulfill these conditions. The five requirements are the following:

(i) *Reduction.* The off-energy-shell amplitude must reduce to the correct on-shell amplitude. In potential theory, this condition is met by fitting the parameters of a given potential model to the experimental value of the on-shell scattering amplitude expressed in terms of phase shifts and mixing parameters.

(ii) *Unitarity.* The amplitude must satisfy off-energy-shell two-particle elastic unitarity. If the amplitude is generated from a potential by the Lippmann-Schwinger equation, this requirement is automatically fulfilled.

(iii) *Analyticity.* The off-energy-shell amplitude $T_{ll'}(p,p';E)$ should be an analytic function of the c.m. kinetic energy E, with the only singularities in E being the right-hand unitarity cut and bound state or resonance poles. It should be analytic in the c.m. momentum $p(p')$ when $p^2>0$ $(p'^2>0)$ and it should have singularities when $p^2<0$ and $p'^2<0$, which become the left-hand or driving singularities of the on-shell amplitude when p and p' are on the energy shell. In addition, we take the position that the on-shell analyticity properties of any model scattering amplitude should be as close as possible to the analytic properties known from relativistic theory.[2] In the nucleon-nucleon case, this means that the on-shell amplitude should have driving singularities *only* for real negative values of E.

(iv) *Time-reversal invariance.*

(v) *Proper threshold behavior.*

We shall see that requirements (iii), (iv), and (v) can be met by a judicious choice of the functional form of the separable potential which generates the scattering amplitude.

Tabakin[3] has done an earlier fit to nucleon-nucleon scattering data, using a separable potential of the same general form as ours. It was the success of the Tabakin potential in a number of calculations which prompted the more extensive fits presented herein.

We will display three different separable-potential fits to the nucleon-nucleon scattering data between 0 and 400 MeV and discuss their application to the study of the qualitative off-energy-shell behavior of partial-wave amplitudes. It would be a most unlikely coincidence if a particular separable-potential model were to reproduce exactly the scattering amplitude which occurs in nature. However, Noyes[4] has shown that the usual local potential models are *not* adequate to explain the observed nucleon-nucleon scattering amplitude. Therefore, a potential model description of the nucleon-nucleon interaction *must* employ a nonlocal potential. Nonlocal separable potentials are the simplest type of nonlocal potentials, they are *very* convenient, and we may hope that they give a good approximation to the exact off-energy-shell scattering amplitude.

II. BASIC EQUATIONS AND CONVENTIONS

To enhance the utility of our results, we shall set forth in considerable detail the basic equations and conventions used in our work. Generally, we follow the conventions of Goldberger and Watson.[5]

We deal with the nonrelativistic two-particle partial-wave Lippmann-Schwinger equation for nucleon-nucleon

* Work done under auspices of the U. S. Atomic Energy Commission.

[1] Thomas R. Mongan, Lawrence Radiation Laboratory Report No. UCRL-17452, 1967 (unpublished).

[2] M. J. Moravcsik, Rev. Mod. Phys. **39**, 670 (1967).

[3] Frank Tabakin, Ann. Phys. (N. Y.) **30**, 51 (1964).

[4] H. P. Noyes, SLAC-PUB-256, 1967 (unpublished), paper presented at the International Colloquium on Polarized Targets and Beams, C.E.N., Saclay, France, 1966.

[5] M. Goldberger and K. Watson, *Collision Theory* (John Wiley & Sons, Inc., New York, 1964).

scattering, which for uncoupled waves is

$$T_l(p,p';k^2)=V_l(p,p')+\frac{2\mu}{\hbar^2}\int_0^\infty \frac{q^2dqV_l(p,q)T_l(q,p';k^2)}{k^2-q^2+i\epsilon}, \quad (1)$$

where the c.m. kinetic energy $E=\hbar^2k^2/2\mu$ and μ is the reduced mass of the two nucleons. For coupled waves, the Lippmann-Schwinger equation is

$$T_{ll'}(p,p';k^2)=V_{ll'}(p,p')+\frac{2\mu}{\hbar^2}\sum_{i=J-1}^{J+1}\int_0^\infty \frac{q^2dqV_{lj}(p,q)T_{jl'}(q,p';k^2)}{k^2-q^2+i\epsilon}. \quad (2)$$

The partial-wave transition amplitude or T matrix obtained from the Lippmann-Schwinger equation satisfies the off-energy-shell elastic two-particle unitarity relation in the form

$$\mathrm{Im}T_l(p,p';k^2)=-\pi\rho_E T_l(p,k;k^2)T_l^*(k,p';k^2) \quad (3)$$

for uncoupled waves and

$$\mathrm{Im}T_{ll'}(p,p';k^2)=-\pi\rho_E\sum_{i=J-1}^{J+1}T_{li}(p,k;k^2)T_{il}^*(k,p';k^2) \quad (4)$$

for coupled waves, where $\rho_E=\mu k/\hbar^2$. We have used time-reversal invariance to cast the unitarity relation in the forms (3) and (4).

The partial-wave S matrix is related to the partial-wave T matrix by

$$S_{ll'}(k^2)=1-2\pi i\rho_E T_{ll'}(k^2). \quad (5)$$

For uncoupled waves $S_l(k^2)=S_{ll}(k^2)$ and the S matrix is expressed in terms of the phase shifts by

$$S_l(k^2)=e^{2i\delta_l(k^2)} \quad (6)$$

or

$$S_l(k^2)=1+2ie^{i\delta_l(k^2)}\sin\delta_l(k^2).$$

Combining (5) and (6) gives

$$\tan2\delta_l(k^2)=\frac{-2\pi\rho_E\,\mathrm{Re}T_l(k^2)}{1+2\pi\rho_E\,\mathrm{Im}T_l(k^2)}.$$

Alternatively, we can express the T matrix in terms of the phase shifts as

$$T_l(k^2)=-(1/\pi\rho_E)e^{i\delta_l(k^2)}\sin\delta_l(k^2),$$

whence

$$\tan\delta_l(k^2)=\mathrm{Im}T_l(k^2)/\mathrm{Re}T_l(k^2).$$

For coupled waves, we use the Stapp[6] parametrization of the S matrix

$$S=\begin{pmatrix}\cos2\epsilon\, e^{2i\delta_{J-1}} & i\sin2\epsilon\, e^{i(\delta_{J-1}+\delta_{J+1})}\\ i\sin2\epsilon\, e^{i(\delta_{J-1}+\delta_{J+1})} & \cos2\epsilon\, e^{2i\delta_{J+1}}\end{pmatrix}.$$

Then, the coupled-wave phase shifts and mixing parameters are given in terms of the T-matrix elements by

$$\tan2\delta_{J-1}=\frac{-2\pi\rho_E\,\mathrm{Re}T_{J-1,J-1}(k^2)}{1+2\pi\rho_E\,\mathrm{Im}T_{J-1,J-1}(k^2)},$$

$$\tan2\delta_{J+1}=\frac{-2\pi\rho_E\,\mathrm{Re}T_{J+1,J+1}(k^2)}{1+2\pi\rho_E\,\mathrm{Im}T_{J+1,J+1}(k^2)},$$

$$\sin2\epsilon=\frac{-2\pi\rho_E\,\mathrm{Re}T_0}{\cos(\delta_{J+1}+\delta_{J-1})},$$

where

$$T_0(k^2)=T_{J-1,J+1}(k^2)=T_{J+1,J-1}(k^2).$$

We consider a separable potential model of the nucleon-nucleon interaction in which

$$V_{ll'}(p,p')=[i^{(l'-l)}][g_l(p)g_{l'}(p')-h_l(p)h_{l'}(p')]. \quad (7)$$

This is *not* a complex potential, since $l'-l$ is zero or two in the nucleon-nucleon case, and the factor $i^{(l'-l)}$ is included merely to change the sign of the off-diagonal elements of the potential matrix in the coupled-wave case.

For uncoupled waves in which we have a single-term separable potential $V_l(p,p')=\lambda g_l(p)g_l(p')$, we find

$$T_l(p,p';k^2)=\lambda g_l(p)g_l(p')\Big/\left(1-\frac{2\mu\lambda}{\hbar^2}\int_0^\infty\frac{dqq^2g_l^2(q)}{k^2-q^2+i\epsilon}\right), \quad (8)$$

where $\lambda=+1$ gives a repulsive potential and $\lambda=-1$ gives an attractive potential. For a two-term separable potential in uncoupled waves we find

$$T_l(p,p';k^2)=N_l(p,p';k^2)/D_l(k^2), \quad (9)$$

where

$$N_l(p,p';k^2)=g_l(p)g_l(p')\left(1+\frac{2\mu}{\hbar^2}\int_0^\infty\frac{dqq^2h_l^2(q)}{k^2-q^2+i\epsilon}\right)-h_l(p)h_l(p')\left(1-\frac{2\mu}{\hbar^2}\int_0^\infty\frac{dqq^2g_l^2(q)}{k^2-q^2+i\epsilon}\right)-[g_l(p)h_l(p')+h_l(p)g_l(p')]\times\frac{2\mu}{\hbar^2}\int_0^\infty\frac{dqq^2g_l(q)h_l(q)}{k^2-q^2+i\epsilon}$$

and

$$D_l(k^2)=\left(1-\frac{2\mu}{\hbar^2}\int_0^\infty\frac{dqq^2g_l^2(q)}{k^2-q^2+i\epsilon}\right)\times\left(1+\frac{2\mu}{\hbar^2}\int_0^\infty\frac{dqq^2h_l^2(q)}{k^2-q^2+i\epsilon}\right)+\left(\frac{2\mu}{\hbar^2}\int_0^\infty\frac{dqq^2g_l(q)h_l(q)}{k^2-q^2+i\epsilon}\right)^2.$$

[6] H. P. Stapp, T. J. Ypsilantis, and N. Metropolis, Phys. Rev. 105, 302 (1957).

In the general case of coupled waves, insertion of the potential (7) into the Lippmann-Schwinger equation (2) yields

$$T_{ll'}(p,p';k^2)=i^{(l'-l)}N_{ll'}(p,p';k^2)/D_J(k^2), \quad (10)$$

where

$$N_{ll'}(p,p';k^2)$$
$$=g_l(p)g_{l'}(p')\left(1+\frac{2\mu}{\hbar^2}\sum_{j=J-1}^{J+1}\int_0^\infty\frac{dqq^2h_j^2(q)}{k^2-q^2+i\epsilon}\right)$$
$$-h_l(p)h_{l'}(p')\left(1-\frac{2\mu}{\hbar^2}\sum_{j=J-1}^{J+1}\int_0^\infty\frac{dqq^2g_j^2(q)}{k^2-q^2+i\epsilon}\right)$$
$$-[g_l(p)h_{l'}(p')+h_l(p)g_{l'}(p')]$$
$$\times\frac{2\mu}{\hbar^2}\sum_{j=J-1}^{J+1}\int_0^\infty\frac{dqq^2g_j(q)h_j(q)}{k^2-q^2+i\epsilon}$$

and

$$D_J(k^2)=\left(1-\frac{2\mu}{\hbar^2}\sum_{j=J-1}^{J+1}\int_0^\infty\frac{dqq^2g_j^2(q)}{k^2-q^2+i\epsilon}\right)$$
$$\times\left(1+\frac{2\mu}{\hbar^2}\sum_{j=J-1}^{J+1}\int_0^\infty\frac{dqq^2h_j^2(q)}{k^2-q^2+i\epsilon}\right)$$
$$+\left(\frac{2\mu}{\hbar^2}\sum_{j=J-1}^{J+1}\int_0^\infty\frac{dqq^2g_j(q)h_j(q)}{k^2-q^2+i\epsilon}\right)^2.$$

For $J=1$, the triplet scattering length a_t, the triplet effective range r_t, and the deuteron binding energy are related by[7]

$$r_t=(2/k_D)(1-1/a_tk_D), \quad (11)$$

where the deuteron binding energy is $E_D=\hbar^2k_D^2/2\mu$. In the $^1S_0$ partial wave, the position of the singlet antibound state (or virtual state) is related to the singlet effective range and the singlet scattering length by

$$k_V=\{1-[1-(2r_s/a_s)]^{1/2}\}/r_s. \quad (12)$$

The singlet antibound state occurs at $E_V=-\hbar^2k_V^2/2\mu$ on the *second* or unphysical sheet of the complex-energy Riemann surface, because the experimental values of a_s and r_s lead to a negative value of k_V in Eq. (12).[8]

The scattering lengths are obtained from the T matrix as follows:

$$a_s=\lim_{k\to0}-\frac{\pi}{2}\frac{2\mu}{\hbar^2}\mathrm{Re}T_0(k^2),$$

$$a_t=\lim_{k\to0}-\frac{\pi}{2}\frac{2\mu}{\hbar^2}\mathrm{Re}T_{00}(k^2),$$

where $T_0(k^2)$ is the transition amplitude for $^1S_0$ scattering and $T_{00}(k^2)$ is the transition matrix element for $J=1$, $l=l'=0$.

The Schrödinger equation in momentum space for the deuteron wave function is

$$\psi_D(\mathbf{k})=-\frac{2\mu}{\hbar^2}\frac{1}{k^2+k_D^2}\int V(\mathbf{k},\mathbf{k}')\psi_D(\mathbf{k}')d^3k', \quad (13)$$

where $(\hbar k_D)^2/2\mu$ is the deuteron binding energy. We write the deuteron wave function as

$$\psi_D(\mathbf{k})=\sum_{l=J-1}^{J+1}w_{\alpha l}(k)\Phi_{1Ml}(\theta_k,\phi_k,1) \quad (14)$$

and the potential as

$$V(\mathbf{k},\mathbf{k}')=\sum_{JSll'M}V_{ll'}(k,k')\Phi_{JMl}(\hat{k},S)\Phi_{JMl'}{}^*(\hat{k}',S), \quad (15)$$

where $\Phi_{JMl}(\theta,\phi,S)$ are the normalized eigenfunctions of J, $J_z=M$ and l given by Hulthén and Sugawara[9] and α denotes the quantum numbers $J=1$, $I=0$, $S=1$ of the deuteron. Combining (13)–(15), we obtain the Schrödinger equation for the "radial" part of the deuteron wave function in momentum space,

$$w_{\alpha l}(k)=-\frac{2\mu}{\hbar^2}\frac{1}{k^2+k_D^2}\int_0^\infty\sum_{l'}V_{ll'}(k,k')w_{\alpha l'}(k')k'^2dk'.$$

Using the potential (7), we find

$$w_{\alpha l}(k)=-\frac{2\mu}{\hbar^2}\frac{i^{-l}}{k^2+k_D^2}[Ag_l(k)-Bh_l(k)],$$

where the normalization constants A and B are given by

$$B=\left(\frac{1+G}{M}\right)A,$$

$$A=\frac{\hbar^2}{2\mu}\Bigg[\sum_{l=J-1}^{J+1}\int_0^\infty\frac{g_l^2(k)k^2dk}{(k^2+k_D^2)^2}$$
$$-2\left(\frac{1+G}{M}\right)\sum_{l=J-1}^{J+1}\int_0^\infty\frac{g_l(k)h_l(k)k^2dk}{(k^2+k_D^2)^2}$$
$$+\left(\frac{1+G}{M}\right)^2\sum_{l=J-1}^{J+1}\int_0^\infty\frac{h_l^2(k)k^2dk}{(k^2+k_D^2)^2}\Bigg]^{-1/2},$$

with

$$G=\frac{2\mu}{\hbar^2}\sum_{l=J-1}^{J+1}\int_0^\infty\frac{g_l^2(k)k^2dk}{k^2+k_D^2},$$

$$M=\frac{2\mu}{\hbar^2}\sum_{l=J-1}^{J+1}\int_0^\infty\frac{g_l(k)h_l(k)k^2dk}{k^2+k_D^2}.$$

[7] H. P. Noyes, Phys. Rev. **130**, 2025 (1963).

[8] S. T. Ma, Rev. Mod. Phys. **25**, 853 (1953). We use the term "antibound" state as proposed by Regge in *Theoretical Physics* (International Atomic Energy Agency, Vienna, 1963).

[9] Lamek Hulthén and Masao Sugawara, in *Handbuch der Physik* (Springer-Verlag, Berlin, 1957), Vol. 39, p. 1.

The normalization is

$$\int \psi_D^*(\mathbf{k})\psi_D(\mathbf{k})d^3k = \sum_{l=J-1}^{J+1} \int_0^\infty k^2 dk w_{\alpha l}^2(k) = 1,$$

whence the deuteron D state probability is

$$P_D = \int_0^\infty k^2 dk w_{\alpha 2}^2(k).$$

Taking the Fourier transform of the deuteron wave function according to

$$\psi_D(\mathbf{r}) = \frac{1}{[(2\pi)^3]^{1/2}} \int \psi_D(\mathbf{k}) e^{i\mathbf{k}\cdot\mathbf{r}} d^3k,$$

we find

$$\psi_D(\mathbf{r}) = \frac{1}{r} \sum_{l=J-1}^{J+1} u_{\alpha l}(r)\Phi_{1Ml}(\theta_r,\phi_r,1),$$

where

$$u_{\alpha l}(r)/r = \left(\frac{2}{\pi}\right)^{1/2} \int_0^\infty i^l w_{\alpha l}(k) j_l(kr) k^2 dk.$$

The normalization of $w_{\alpha l}(k)$ insures the normalization

$$\sum_{l=J-1}^{J+1} \int_0^\infty u_{\alpha l}^2(r) dr = 1.$$

The deuteron quadrupole moment is given in terms of these radial wave functions by[9]

$$Q = \frac{\sqrt{2}}{10} \int_0^\infty r^2 u_{\alpha 0}(r) u_{\alpha 2}(r) dr - \frac{1}{20} \int_0^\infty r^2 [u_{\alpha 2}(r)]^2 dr.$$

In momentum space, this formula becomes

$$Q = -\frac{\sqrt{2}}{10} \int_0^\infty k^2 w_{\alpha 2}(k) \left(\frac{d^2}{dk^2} w_{\alpha 0}(k) - \frac{1}{k} \frac{d}{dk} w_{\alpha 0}(k) \right) dk$$
$$- \frac{1}{20} \int_0^\infty \left[6 w_{\alpha 2}^2(k) + k^2 \left(\frac{d}{dk} w_{\alpha 2}(k) \right)^2 \right] dk.$$

We take for the nucleon mass M the average of the neutron and proton masses so $2\mu c^2 = Mc^2 = 938.903$ MeV and $\hbar c = 197.32$ MeV F.[10] We take the deuteron binding energy $E_D = 2.22452$ MeV and the triplet scattering length $a_t = 5.396$ F, which yields a triplet effective range $r_t = 1.726$ F.[7] We set the singlet antibound state at an energy $E_V = -0.0665$ MeV on the second sheet of the complex-energy Riemann surface and we take the singlet scattering length $a_s = -23.678$ F. This yields a singlet effective range $r_s = 2.729$ F.

We have fitted our potentials to the Arndt-MacGregor nucleon-nucleon phase shifts obtained at Livermore. We fit all partial waves through $J = 4$. According to the standard impact-parameter argument,[11] the partial wave $l = 5$ does not contribute significantly to nucleon-nucleon scattering below a kinetic energy of about 500 MeV. We believe that our fits should be useful for energies up to 400 MeV and certainly for all energies below the meson production threshold at 270 MeV.

III. POTENTIAL SHAPES

Although the unitarity requirement for off-energy-shell scattering amplitudes is automatically met in the Lippmann-Schwinger formulation of potential scattering theory, and reduction to the correct on-shell amplitude is guaranteed by choosing the potential parameters suitably, the requirements of time-reversal invariance, analyticity, and correct threshold behavior must be satisfied by proper choice of the functional form of the separable potential.

Time-reversal invariance is ensured by our separable potential (7). Therefore we must satisfy the analyticity and threshold requirements by building them into the form factors $g_l(p)$ and $h_l(p)$. Note that different functional forms for these form factors lead to different off-energy-shell behavior and different high-energy behavior of the phase shifts.

We know that the on-shell partial-wave amplitudes must go to zero as $(k^2)^l$ when $k^2 \to 0$, where $E = \hbar^2 k^2/2\mu$ is the kinetic energy. To obtain the correct threshold behavior, Eqs. (8)–(10) show that we must have $h_l(p) \sim p^l$ and $g_l(p) \sim (p)^l$ as $p^2 \to 0$. In addition, we will demand that $g_l(p)$ and $h_l(p)$ have singularities only for p^2 real and negative, so that our model scattering amplitudes will have analyticity properties as close as possible to those of the true nucleon-nucleon scattering amplitude on the energy shell.

In the following work we consider the family of form-factor shapes $f_l(p) \sim p^l/(p^2+a^2)^{(l+n)/2}$, which behave as $f_l(p) \sim p^l$ when $p^2 \to 0$ and have a singularity at $p^2 = -a^2$. Furthermore, $f_l(p) \sim p^{-n}$ as $p^2 \to \infty$.

We also consider the form

$$f_l(p) = \left[\frac{G^2}{\pi p^2} Q_l\left(1 + \frac{\mu^2}{2p^2}\right) \right]^{1/2},$$

where $Q_l(x)$ is the Legendre function of the second kind, which was first proposed by Mitra.[12] This form has the correct threshold behavior and goes as $[(\ln p^2)/p^2]^{1/2}$ as $p^2 \to \infty$. The on-shell Born approximation to the transition amplitude obtained from a separable potential with this Mitra form factor is identical to that arising from a superposition of Yukawa potentials. In addition, the Mitra form factor leads to an on-shell transition amplitude which has a cut along the negative real energy axis, beginning at $k^2 = -\frac{1}{4}\mu^2$. Thus this last

[10] A. Rosenfeld *et al.*, Rev. Mod. Phys. **39**, 1 (1967).

[11] Michael J. Moravcsik, *The Two-Nucleon Interaction* (Clarendon Press, Oxford, England, 1963), p. 37.

[12] A. N. Mitra, Phys. Rev. **123**, 1892 (1961).

TABLE I. Case-I fits to nucleon-nucleon phase shifts in uncoupled partial waves. These partial waves are fitted by the separable potential

$$V_l(p,p')=g_l(p)g_l(p')-h_l(p)h_l(p'),$$

where the form factors are

$$g_l(p)=C_R p^l/(p^2+a_R^2)^{(l+1)/2}, \quad h_l(p)=C_A p^l/(p^2+a_A^2)^{(l+1)/2},$$

except in the partial waves $^1S_0$ and $^3P_0$, where the repulsive form factor is

$$g_l^R(p)=C_R p^{l+2}/(p^2+a_R^2)^{(l+3)/2}.$$

The units of the attractive inverse range a_A and the repulsive inverse range a_R are inverse fermis (F^{-1}, 1 F = 10^{-13} cm). The units of the attractive coupling strength C_A and the repulsive coupling strength C_R are (MeV F)$^{1/2}$. Dots indicate that a form factor is to be set equal to zero. $\sum R^2$ is the sum of the squares of the residuals,

$$\sum R^2 \equiv \sum_{i=1}^{50} [\delta_l{}^{\text{expt}}(E_i)-\delta_l{}^{\text{fit}}(E_i)]^2,$$

over the 50 data spaced at 8-MeV intervals in the range 0–400 MeV.

Partial wave	Repulsive potential parameters a_R (F^{-1})	C_R [(MeV F)$^{1/2}$]	Attractive potential parameters a_A (F^{-1})	C_A [(MeV F)$^{1/2}$]	ΣR^2
Singlet					
$^1S_0$	2.1[a]	500.0[a]	0.786	5.420	698.2
$^1P_1$	1.539	100.0	...	...	596.9
$^1D_2$	...	...	1.456	4.931	8.972
$^1F_3$	0.544	1.491	...	...	0.708
$^1G_4$	...	...	0.990	1.979	0.0893
Triplet					
$^3P_0$	1.64[a]	100.0[a]	0.957	5.415	81.83
$^3P_1$	1.574	19.64	...	...	38.39
$^3D_2$	...	...	1.059	5.784	36.32
$^3F_3$	0.849	2.410	...	...	0.0871
$^3G_4$	...	...	1.085	4.555	4.205

[a] Special repulsive form factor must be used.

separable-potential form has more realistic analyticity properties than the preceding forms.

IV. FITS TO NUCLEON-NUCLEON DATA

We have fit the Arndt-MacGregor (Livermore) nucleon-nucleon phase shifts for laboratory kinetic energy from 0 to 400 MeV for the partial waves through $J=4$.

The fitting was done on a CDC-6600 electronic computer at Lawrence Radiation Laboratory using a least-squares minimization program LSQMIN developed by Eric Beals. For each phase parameter we used 50 data points at 8-MeV intervals in the range 0–400 MeV laboratory kinetic energy E. The program LSQMIN searches for the values of the potential parameters which minimize the sum of the squares of the residuals

$$\sum R^2 = \sum_{i=1}^{50} [\delta_l{}^{\text{expt}}(E_i)-\delta_l{}^{\text{fit}}(E_i)]^2$$

for uncoupled waves, and

$$\sum R^2 = \sum_{i=1}^{50} [\delta_{J-1}{}^{\text{expt}}(E_i)-\delta_{J-1}{}^{\text{fit}}(E_i)]^2 + \sum_{i=1}^{50} [\epsilon_J{}^{\text{expt}}(E_i)-\epsilon_J{}^{\text{fit}}(E_i)]^2 + \sum_{i=1}^{50} [\delta_{J+1}{}^{\text{expt}}(E_i)-\delta_{J+1}{}^{\text{fit}}(E_i)]^2$$

for coupled waves.

All of our fits were made with the basic separable potential form

$$V_{ll'}(p,p')=[i^{(l'-l)}][g_l(p)g_{l'}(p')-h_l(p)h_{l'}(p')].$$

An attempt was made to fit all the scattering data by using three of the form factors mentioned in Sec. III. In case I, $g_l(p)$ and $h_l(p)$ were taken as $Cp^l/(p^2+a^2)^{(l+1)/2}$. In case II, $g_l(p)$ and $h_l(p)$ were of the form $Cp^l/(p^2+a^2)^{(l+2)/2}$. These shapes correspond to the first two members $n=1$ and $n=2$ of the family of form-factor shapes discussed in Sec. III. Finally, in case III, $g_l(p)$

TABLE II. Case-II fits to nucleon-nucleon phase shifts in uncoupled partial waves. These partial waves are fitted by the separable potential

$$V_l(p,p')=g_l(p)g_l(p')-h_l(p)h_l(p'),$$

where the form factors are

$$g_l(p)=C_R p^l/(p^2+a_R^2)^{(l+2)/2}, \quad h_l(p)=C_A p^l/(p^2+a_A^2)^{(l+2)/a},$$

except in the partial waves $^1S_0$ and $^3P_0$, where the repulsive form factor is

$$g_l^R(p)=C_R p^{l+2}/(p^2+a_R^2)^{(l+4)/2}.$$

The units of the attractive inverse range a_A and the repulsive inverse range a_R are inverse fermis (F^{-1}, 1 F = 10^{-13} cm). The units of the attractive coupling strength C_A and the repulsive coupling strength C_R are (MeV/F)$^{1/2}$. Dots indicate that a form factor is to be set equal to zero. $\sum R^2$ is the sum of the squares of the residuals,

$$\sum R^2 = \sum_{i=1}^{50} [\delta_l{}^{\text{expt}}(E_i)-\delta_l{}^{\text{fit}}(E_i)]^2,$$

over the 50 data spaced at 8-MeV intervals in the range 0–400 MeV.

Partial wave	Repulsive potential parameters a_R (F^{-1})	C_R [(MeV/F)$^{1/2}$]	Attractive potential parameters a_A (F^{-1})	C_A [(MeV/F)$^{1/2}$]	ΣR^2
Singlet					
$^1S_0$	3.874[a]	679.3[a]	0.991	7.049	1284.8
$^1P_1$	2.951	500.0	...	...	76.94
$^1D_2$	...	...	1.986	21.98	14.55
$^1F_3$	0.906	3.926	...	...	0.157
$^1G_4$	...	...	1.333	6.982	0.251
Triplet					
$^3P_0$	2.527[a]	330.2[a]	1.117	8.348	5.674
$^3P_1$	2.177	43.87	...	...	55.47
$^3D_2$	...	...	1.566	23.15	147.2
$^3F_3$	1.235	7.574	...	...	0.968
$^3G_4$	...	...	1.439	17.78	8.883

[a] Special repulsive form factor must be used.

TABLE III. Case-III fits to nucleon-nucleon phase shifts in uncoupled partial waves. These partial waves are fitted by the separable potential

$$V_l(p,p')=g_l(p)g_l(p')-h_l(p)h_l(p'),$$

where the form factors are

$$g_l(p)=G_R[(1/\pi p^2)Q_l(1+\mu_R^2/2p^2)]^{1/2},$$
$$h_l(p)=G_A[(1/\pi p^2)Q_l(1+\mu_A^2/2p^2)]^{1/2},$$

except in the partial waves $^1S_0$ and $^3P_0$, where the repulsive form factor is

$$g_l^R(p)=[G_R p^2/(p^2+\tfrac{1}{4}\mu_R^2)][(1/\pi p^2)Q_l(1+\mu_R^2/2p^2)]^{1/2}.$$

The units of the attractive inverse range μ_A and the repulsive inverse range μ_R are inverse fermis (F^{-1}, 1 F$=10^{-13}$ cm). The units of the attractive coupling strength G_A and the repulsive coupling strength G_R are (MeV F)$^{1/2}$. Dots indicate that a form factor is to be set equal to zero. $\sum R^2$ is the sum of the squares of the residuals

$$\sum R^2=\sum_{i=1}^{50}[\delta_l^{\rm expt}(E_i)-\delta_l^{\rm fit}(E_i)]^2,$$

over the 50 data spaced at 8-MeV intervals in the range 0–400 MeV.

Partial wave	Repulsive potential parameters μ_R (F^{-1})	G_R [(MeV F)$^{1/2}$]	Attractive potential parameters μ_A (F^{-1})	G_A [(MeV F)$^{1/2}$]	ΣR^2
Singlet					
$^1S_0$	2.319[a]	21.50[a]	1.203	9.416	1805.9
$^1P_1$	0.931	465.7	···	···	2406.1
$^1D_2$	···	···	1.453	10.86	3.434
$^1F_3$	0.330	2.645	···	···	2.562
$^1G_4$	···	···	0.820	5.316	0.0018
Triplet					
$^3P_0$	1.800[a]	200.0[a]	1.550	29.00	386.7
$^3P_1$	1.193	500.0	···	···	187.6
$^3D_2$	···	···	0.912	10.49	3.884
$^3F_3$	0.666	5.583	···	···	0.216
$^3G_4$	···	···	0.926	11.48	0.573

[a] Special repulsive form factor must be used.

and $h_l(p)$ were taken to be of the Mitra form

$$\left[\frac{G^2}{\pi p^2}Q_l\left(1+\frac{\mu^2}{2p^2}\right)\right]^{1/2}.$$

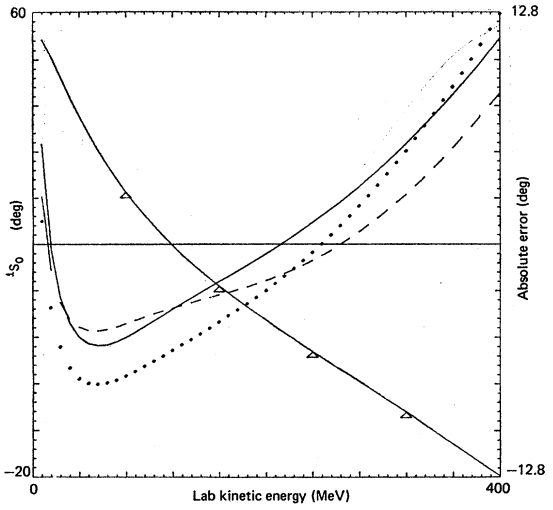

FIG. 1. Fits to the singlet phase shift $^1S_0$ with special repulsive form factors. The curve marked △ is the data value of the phase parameter in degrees and is read with the left-hand scale. The other curves are the absolute error (fitted value minus data value) in degrees of the various fits and are read with the right-hand scale. The dashed curve represents the case-I fit, the solid curve marks the case-II fit, and the dotted curve indicates the case-III fit.

With this approach, we obtained fits to most of the partial-wave phase shifts. However, in the partial waves $^1S_0$ and $^3P_0$ reasonable fits could be found only if we used the following special repulsive form factors:

$$\text{case I:}\quad g_l^{I,R}(p)=C\frac{p^2}{p^2+a^2}\frac{p^l}{(p^2+a^2)^{(l+1)/2}},$$

$$\text{case II:}\quad g_l^{II,R}(p)=C\frac{p^2}{p^2+a^2}\frac{p^l}{(p^2+a^2)^{(l+2)/2}},$$

$$\text{case III:}\quad g_l^{III,R}(p)=[p^2/(p^2+\tfrac{1}{4}\mu^2)]\left[\frac{G^2}{\pi p^2}Q_l\left(1+\frac{\mu^2}{2p^2}\right)\right]^{1/2}.$$

TABLE IV. Case-I fits to nucleon-nucleon phase parameters in coupled partial waves. These partial waves are fitted by the separable potential $V_{ll'}(p,p')=(i^{l'-l})[g_l(p)g_{l'}(p')-h_l(p)h_{l'}(p')]$, where the form factors are $g_l(p)=C_l{}^R p^l/[p^2+(a_l{}^R)^2]^{(l+1)/2}$, $h_l(p)=C_l{}^A p^l/[p^2+(a_l{}^A)^2]^{(l+1)/2}$, except in the SR fits to the $J=1$ system, where the repulsive form factor for $J-1(l=0)$ is $g_l{}^R=C_l{}^R p^{l+2}/[p^2+(a_l{}^R)^2]^{(l+3)/2}$. The units of the attractive inverse ranges $a_{J+1}{}^A$ and $a_{J-1}{}^A$ and the repulsive inverse ranges $a_{J+1}{}^R$ and $a_{J-1}{}^R$ are inverse fermis (F^{-1}, 1 F$=10^{-13}$ cm). The units of the attractive coupling strengths $C_{J+1}{}^A$ and $C_{J-1}{}^A$ and the repulsive coupling strengths $C_{J+1}{}^R$ and $C_{J-1}{}^R$ are (MeV F)$^{1/2}$. Dots indicate that a form factor is to be set equal to zero. $\sum R^2$ is the sum of the squares of the residuals,

$$\sum R^2\equiv\sum_{i=1}^{50}\{[\delta_{J+1}{}^{\rm expt}(E_i)-\delta_{J+1}{}^{\rm fit}(E_i)]^2+[\epsilon_J{}^{\rm expt}(E_i)-\epsilon_J{}^{\rm fit}(E_i)]^2+[\delta_{J-1}{}^{\rm expt}(E_i)-\delta_{J-1}{}^{\rm fit}(E_i)]^2\},$$

over the 50 data spaced at 8-MeV intervals in the range 0-400 MeV.

Coupled wave system	Parameters for $l=J+1$: Repulsive parameters $a_{J+1}{}^R$ (F^{-1})	$C_{J+1}{}^R$ [(MeV F)$^{1/2}$]	Attractive parameters $a_{J+1}{}^A$ (F^{-1})	$C_{J+1}{}^A$ [(MeV F)$^{1/2}$]	Parameters for $l=J-1$: Repulsive parameters $a_{J-1}{}^R$ (F^{-1})	$C_{J-1}{}^R$ [(MeV F)$^{1/2}$]	Attractive parameters $a_{J-1}{}^A$ (F^{-1})	$C_{J-1}{}^A$ [(MeV F)$^{1/2}$]	$\sum R^2$
$J=1$	0.849	19.57	0.747	10.81	3.836	21.45	0.984	9.754	2271.3
$J=1$ SR	1.059	62.62	0.885	13.07	1.841[a]	59.63[a]	1.416	10.72	1392.7
$J=2$	···	···	0.551	0.727	···	···	1.415	5.010	11.16
$J=3$	1.019	4.347	···	···	0.899	3.342	1.165	4.628	10.25
$J=4$	···	···	0.604	0.776	···	···	1.514	3.964	6.704

[a] Special repulsive form factor must be used.

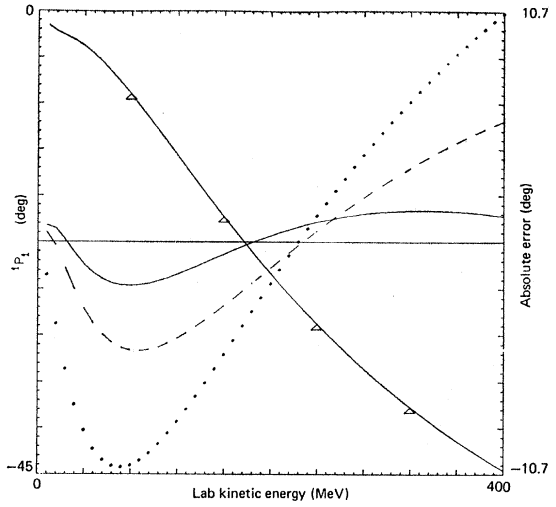

FIG. 2. Fits to the singlet phase shift $^1P_1$. Description of curves is as for Fig. 1.

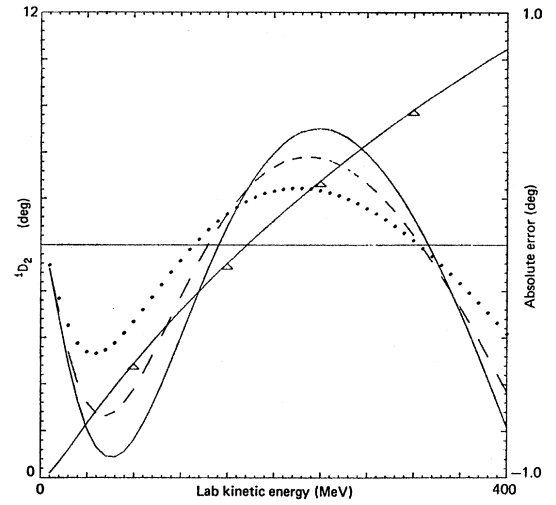

FIG. 3. Fits to the singlet phase shift $^1D_2$. Description of curves is as for Fig. 1.

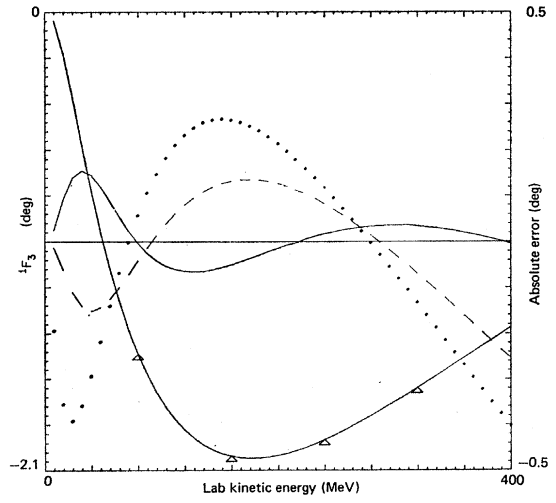

FIG. 4. Fits to the singlet phase shift $^1F_3$. Description of curves is as for Fig. 1.

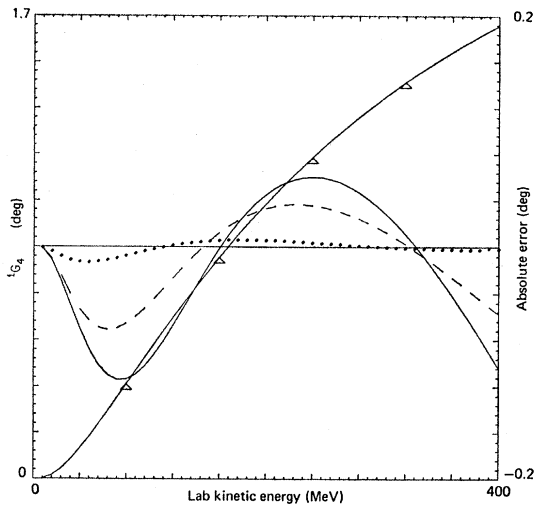

FIG. 5. Fits to the singlet phase shift $^1G_4$. Description of curves is as for Fig. 1.

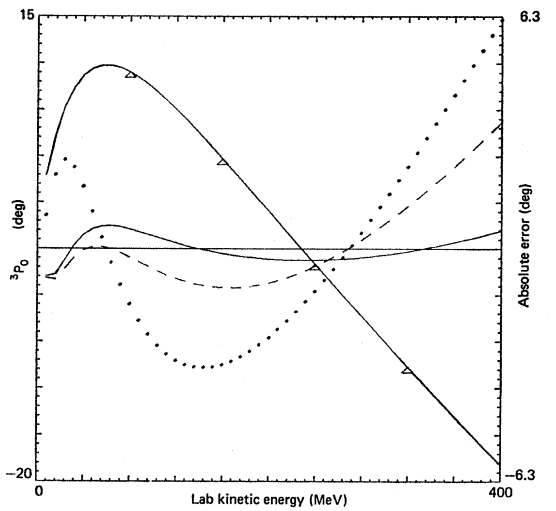

FIG. 6. Fits to the (uncoupled) triplet phase shift $^3P_0$ with special repulsive form factors. Description of curves is as for Fig. 1.

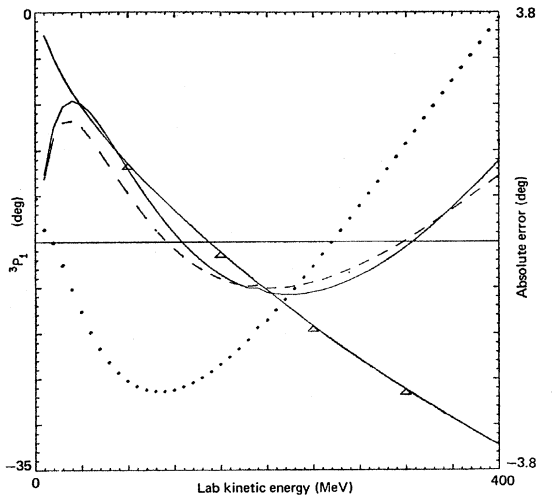

FIG. 7. Fits to the (uncoupled) triplet phase shift $^3P_1$. Description of curves is as for Fig. 1.

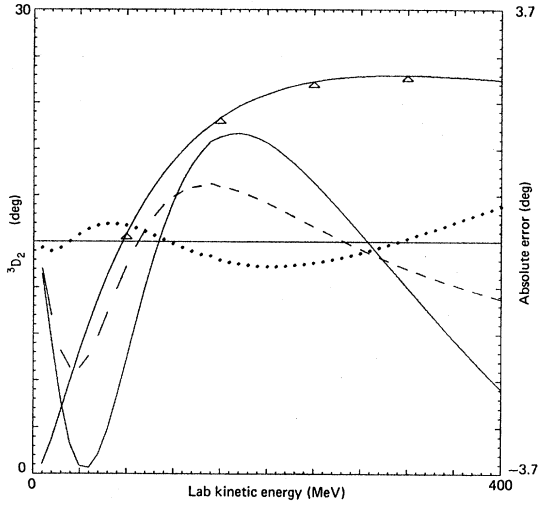

FIG. 8. Fits to the (uncoupled) triplet phase shift $^3D_2$. Description of curves is as for Fig. 1.

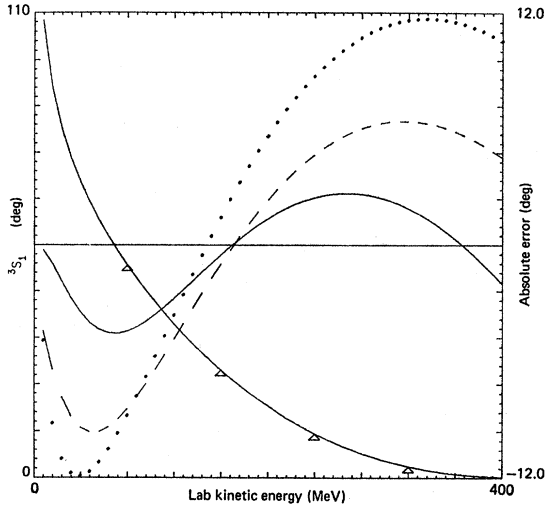

FIG. 11. Fits to the triplet phase shift $^3S_1$ ($J=1$ coupled waves). Description of curves is as for Fig. 1.

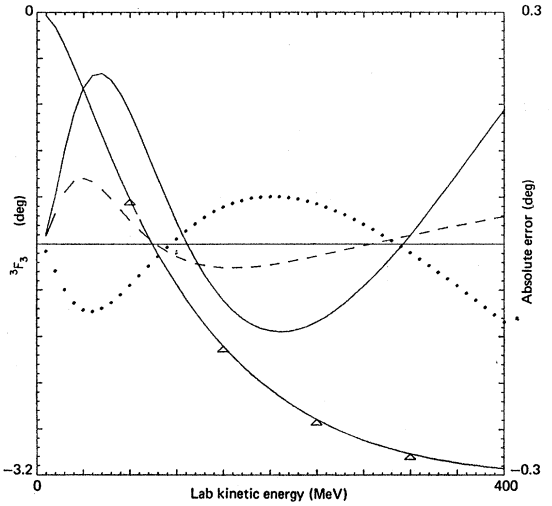

FIG. 9. Fits to the (uncoupled) triplet phase shift $^3F_3$. Description of curves is as for Fig. 1.

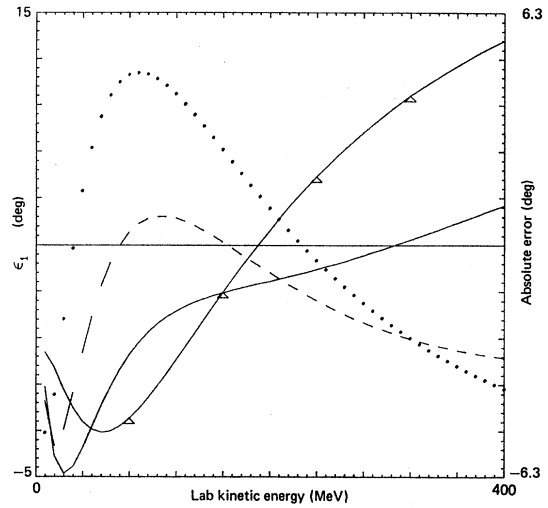

FIG. 12. Fits to the triplet mixing parameter ϵ_1 ($J=1$ coupled waves). Description of curves is as for Fig. 1.

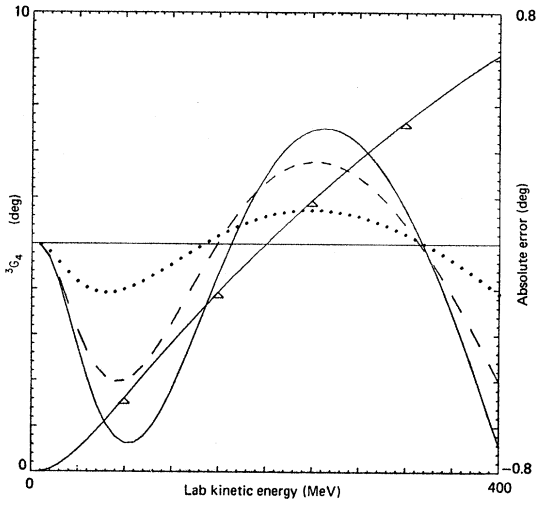

FIG. 10. Fits to the (uncoupled) triplet phase shift $^3G_4$. Description of curves is as for Fig. 1.

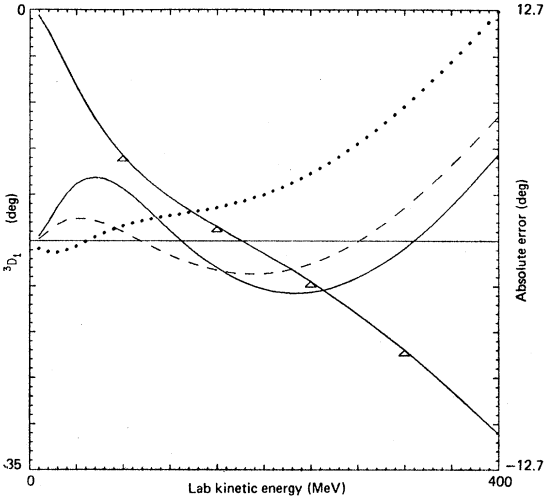

FIG. 13. Fits to the triplet phase shift $^3D_1$ ($J=1$ coupled waves). Description of curves is as for Fig. 1.

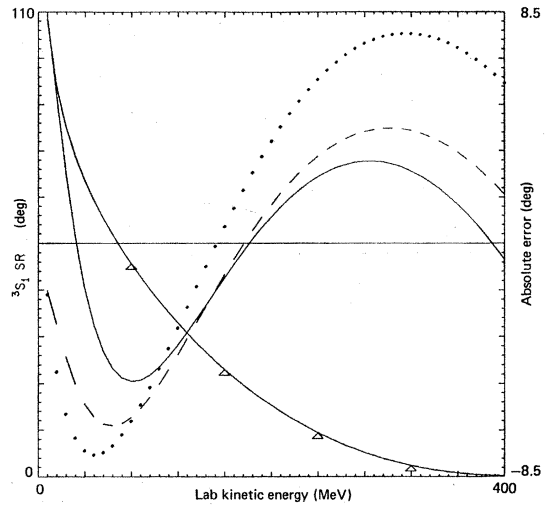

FIG. 14. SR fits to the triplet phase shift $^3S_1$ ($J=1$ coupled waves) with special repulsive form factor in $l=0$. Description of curves is as for Fig. 1.

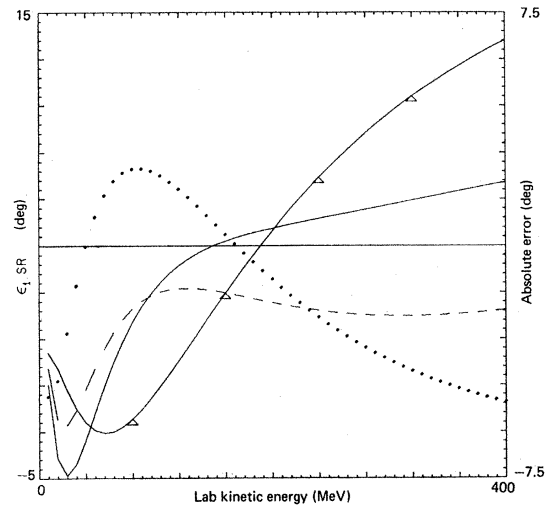

FIG. 15. SR fits to the triplet mixing parameter ϵ_1 ($J=1$ coupled waves) with special repulsive form factor in $l=0$. Description of curves is as for Fig. 1.

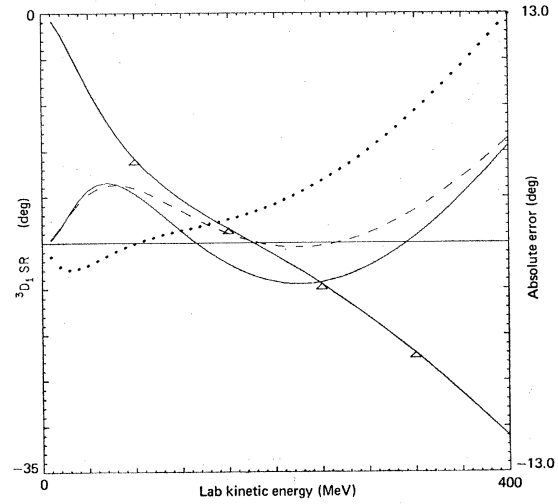

FIG. 16. SR fits to the triplet phase shift $^3D_1$ ($J=1$ coupled waves) with special repulsive form factor in $l=0$. Description of curves is as for Fig. 1.

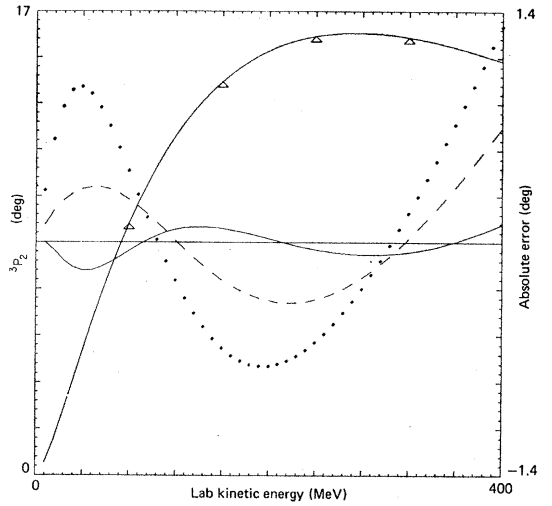

FIG. 17. Fits to the triplet phase shift $^3P_2$ ($J=2$ coupled waves). Description of curves is as for Fig. 1.

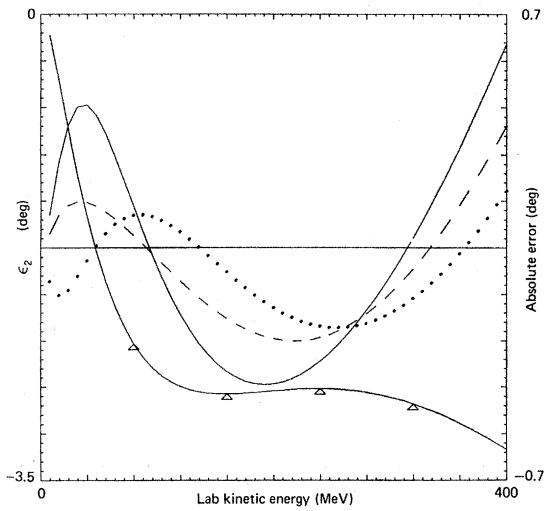

FIG. 18. Fits to the triplet mixing parameters ϵ_2 ($J=2$ coupled waves). Description of curves is as for Fig. 1.

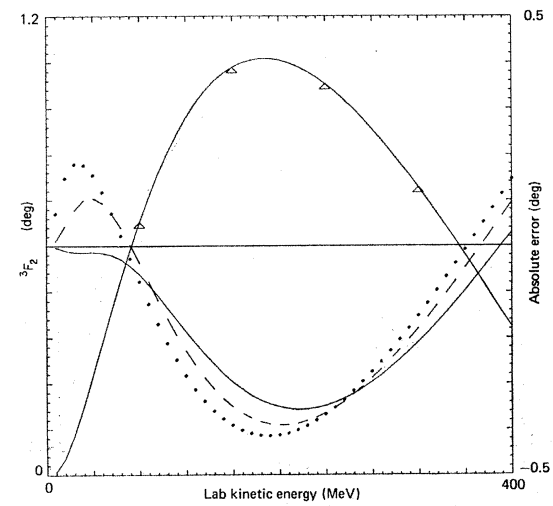

FIG. 19. Fits to the triplet phase shift $^3F_2$ ($J=2$ coupled waves). Description of curves is as for Fig. 1.

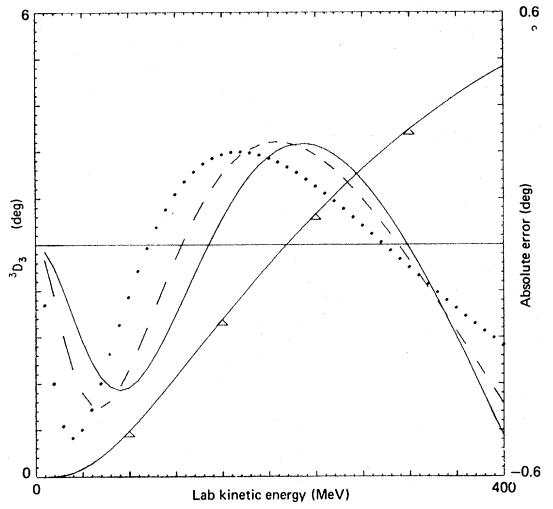

FIG. 20. Fits to the triplet phase shift $^3D_3$ ($J=3$ coupled waves). Description of curves is as for Fig. 1.

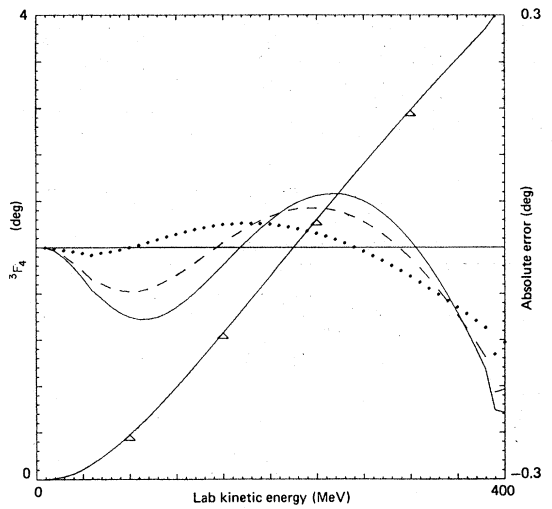

FIG. 23. Fits to the triplet phase shift $^3F_4$ ($J=4$ coupled waves). Description of curves is as for Fig. 1.

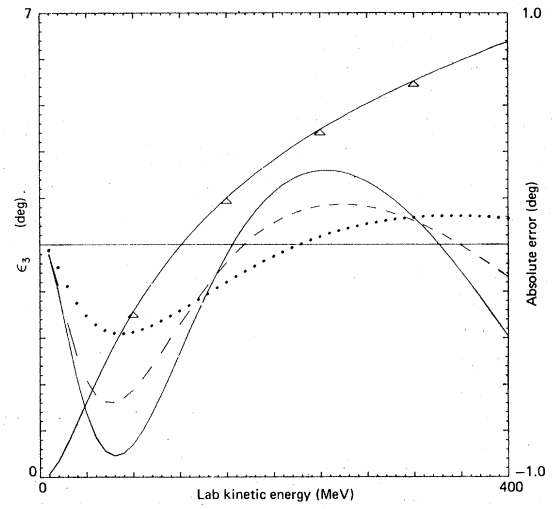

FIG. 21. Fits to the triplet mixing parameter ϵ_3 ($J=3$ coupled waves). Description of curves is as for Fig. 1.

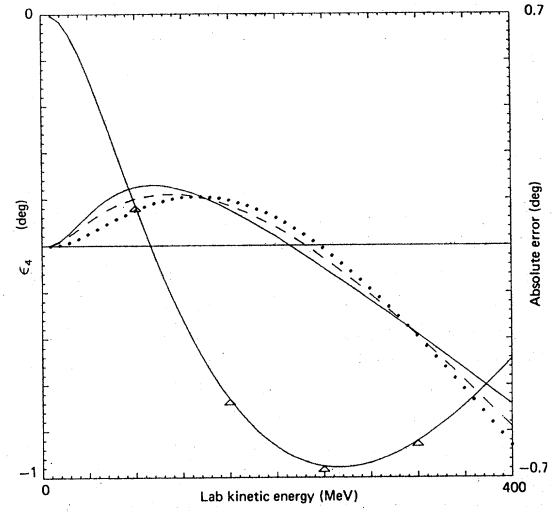

FIG. 24. Fits to the triplet mixing parameter ϵ_4 ($J=4$ coupled waves). Description of curves is as for Fig. 1.

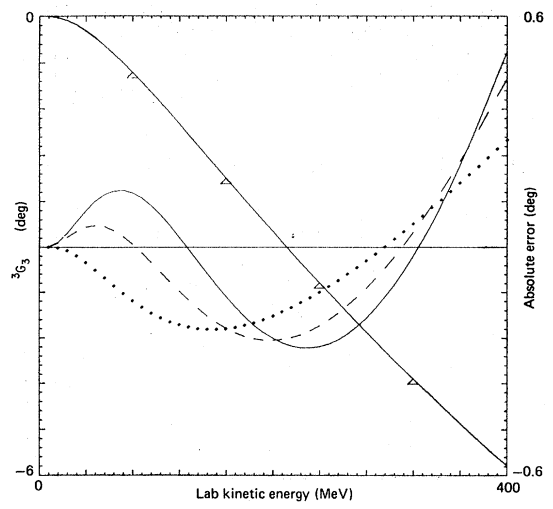

FIG. 22. Fits to the triplet phase shift $^3G_3$ ($J=3$ coupled waves). Description of curves is as for Fig. 1.

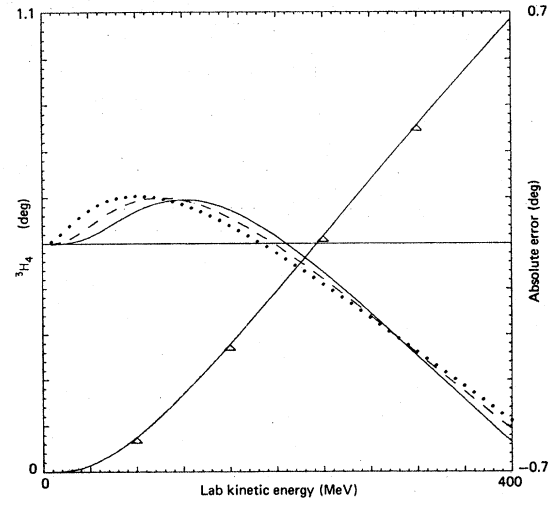

FIG. 25. Fits to the triplet phase shift $^3H_4$ ($J=4$ coupled waves). Description of curves is as for Fig. 1.

TABLE V. Case-II fits to nucleon-nucleon phase parameters in coupled partial waves. These partial waves are fitted by the separable potential $V_{ll'}(p,p')=(i^{l'-l})[g_l(p)g_{l'}(p')-h_l(p)h_{l'}(p')]$, where the form factors are $g_l(p)=C_l{}^R p^l/[p^2+(a_l{}^R)^2]^{(l+2)/2}$, $h_l(p)=C_l{}^A p^l/[p^2+(a_l{}^A)^2]^{(l+2)/2}$, except in the SR fits to the $J=1$ system, where the repulsive form factor for $J-1(l=0)$ is $g_l{}^R(p)=C_l{}^R p^{l+2}/[p^2+(a_l{}^R)^2]^{(l+4)/2}$. The units of the attractive inverse ranges $a_{J+1}{}^R$ and $a_{J-1}{}^A$ and the repulsive inverse ranges $a_{J+1}{}^R$ and $a_{J-1}{}^R$ are inverse fermis (F^{-1}, 1 F$=10^{-13}$ cm). The units of the attractive coupling strengths $C_{J+1}{}^A$ and $C_{J-1}{}^A$ and the repulsive coupling strengths $C_{J+1}{}^R$ and $C_{J-1}{}^R$ are (MeV F)$^{1/2}$. Dots indicate that a form factor is to be set equal to zero. $\sum R^2$ is the sum of the squares of the residuals,

$$\sum R^2 \equiv \sum_{i=1}^{50} \{[\delta_{J+1}{}^{\text{expt}}(E_i)-\delta_{J+1}{}^{\text{fit}}(E_i)]^2+[\epsilon_J{}^{\text{expt}}(E_i)-\epsilon_J{}^{\text{fit}}(E_i)]^2+[\delta_{J-1}{}^{\text{expt}}(E_i)-\delta_{J-1}{}^{\text{fit}}(E_i)]^2\},$$

over the 50 data spaced at 8-MeV intervals in the range 0–400 MeV.

Coupled wave system	Parameters for $l=J+1$: Repulsive parameters $a_{J+1}{}^R$ (F^{-1})	$C_{J+1}{}^R$ [(MeV F)$^{1/2}$]	Attractive parameters $a_{J+1}{}^A$ (F^{-1})	$C_{J+1}{}^A$ [(MeV F)$^{1/2}$]	Parameters for $l=J-1$: Repulsive parameters $a_{J-1}{}^R$ (F^{-1})	$C_{J-1}{}^R$ [(MeV F)$^{1/2}$]	Attractive parameters $a_{J-1}{}^A$ (F^{-1})	$C_{J-1}{}^A$ [(MeV F)$^{1/2}$]	$\sum R^2$
$J=1$	1.283	49.11	1.174	34.07	3.308	81.68	1.979	41.42	866.9
$J=1$ SR	1.410	33.20	0.838	4.760	2.411[a]	60.21[a]	1.288	13.18	1083.6
$J=2$	...	...	0.932	2.134	...	...	2.094	21.83	10.02
$J=3$	1.357	13.92	...	...	1.387	11.46	1.641	17.86	15.74
$J=4$	...	...	0.898	2.330	...	...	1.935	17.45	6.847

[a] Special repulsive form factor must be used.

In case III, this introduces a pole at the beginning of the repulsive force cut in the on-shell amplitude. These special repulsive form factors go to zero as $p^2 \to 0$ faster than the corresponding attractive form factors, while both types of form factor have the same behavior as $p^2 \to \infty$. Therefore, at low energies, the potential will be mainly attractive and will have the correct threshold behavior, and the repulsive potential will become important only at high energies.

We have also used these special repulsive form factors in the $^3S_1$ fit labeled SR and for the $l=0$ repulsion in the fit to the coupled waves $J=1$ which is labeled SR.

The parameters which fit the phase shifts are given in Tables I–VI, and we have included the values of $\sum R^2$ since a comparison of these numbers for a single partial-wave or coupled-wave system $J+1$, $J-1$ gives an indication of the relative goodness of fit of the three types of parametrization. We have displayed our fits to the phase parameters graphically in Figs. 1–25, where the curve marked Δ is the data value of the phase parameter in degrees and is read with the left-hand scale. The other curves are the absolute error (fitted value minus data value) in degrees of the various fits and are read with the right-hand scale. The dashed curve represents the case-I fit, the solid curve marks the case-II fit, and the dotted curve indicates the case-III fit.

We have fit the coupled waves $^3S_1$, $^3P_2$, $^3D_3$, and $^3F_4$, assuming $\epsilon_J=0$ and neglecting δ_{J+1} in each case. Thus one can discard higher partial waves at any point. These results are presented in Tables VII–IX and Figs. 26–30.

In the partial wave $^1S_0$, we must fit the three low-energy parameters [scattering length, virtual (anti-bound) state pole position, and effective range] as well as the phase shift. Only two of these low-energy parame-

TABLE VI. Case-III fits to nucleon-nucleon phase parameters in coupled partial waves. These partial waves are fitted by the separable potential $V_{ll'}(p,p')=(i^{l'-l})[g_l(p)g_{l'}(p')-h_l(p)h_{l'}(p')]$, where the form factors are $g_l(p)=G_l{}^R[(1/\pi p^2)Q_l(1+(\mu_l{}^R)^2/2p^2)]^{1/2}$, $h_l(p)=G_l{}^A[(1/\pi p^2)Q_l(1+(\mu_l{}^A)^2/2p^2)]^{1/2}$, where $Q_l(x)$ is the Legendre function of the second kind. In the SR fits to the $J=1$ system, the repulsive form factor for $J-1(l=0)$ is $g_l{}^R(p)=\{G_l{}^R\, p^2/[p^2+\frac{1}{4}(\mu_l{}^R)^2]\}\{(1/\pi p^2)Q_l[1+(\mu_l{}^R)^2/2p^2]\}^{1/2}$. The units of the attractive inverse ranges $\mu_{J+1}{}^A$ and $\mu_{J-1}{}^A$ and the repulsive inverse ranges $\mu_{J+1}{}^R$ and $\mu_{J-1}{}^R$ are inverse fermis (F^{-1}, 1 F$=10^{-13}$ cm). The units of the attractive coupling strengths $G_{J+1}{}^A$ and $G_{J-1}{}^A$ and the repulsive coupling strengths $G_{J+1}{}^R$ and $G_{J-1}{}^R$ are (MeV F)$^{1/2}$. Dots indicate that a form factor is to be set equal to zero. $\sum R^2$ is the sum of the squares of the residuals,

$$\sum R^2 \equiv \sum_{i=1}^{50} \{[\delta_{J+1}{}^{\text{expt}}(E_i)-\delta_{J+1}{}^{\text{fit}}(E_i)]^2+[\epsilon_J{}^{\text{expt}}(E_i)-\epsilon_J{}^{\text{fit}}(E_i)]^2+[\delta_{J-1}{}^{\text{expt}}(E_i)-\delta_{J-1}{}^{\text{fit}}(E_i)]^2\},$$

over the 50 data spaced at 8-MeV intervals in the range 0–400 MeV.

Coupled wave system	Parameters for $l=J+1$: Repulsive parameters $\mu_{J+1}{}^R$ (F^{-1})	$G_{J+1}{}^R$ [(MeV F)$^{1/2}$]	Attractive parameters $\mu_{J+1}{}^A$ (F^{-1})	$G_{J+1}{}^A$ [(MeV F)$^{1/2}$]	Parameters for $l=J-1$: Repulsive parameters $\mu_{J-1}{}^R$ (F^{-1})	$G_{J-1}{}^R$ [(MeV F)$^{1/2}$]	Attractive parameters $\mu_{J-1}{}^A$ (F^{-1})	$G_{J-1}{}^A$ [(MeV F)$^{1/2}$]	$\sum R^2$
$J=1$	0.617	49.81	0.507	16.51	5.502	52.32	0.974	13.42	6027.4
$J=1$ SR	0.594	145.5	0.512	17.47	3.276[a]	145.3[a]	1.320	13.31	3737.6
$J=2$	...	...	0.334	1.163	...	...	1.446	8.942	28.52
$J=3$	0.887	16.84	...	...	0.655	6.814	1.055	9.246	6.132
$J=4$	...	...	0.360	1.463	...	...	1.546	11.33	6.668

[a] Special repulsive form factor must be used.

ters are independent and we choose the scattering length to be -23.678 F and the antibound pole at $E_V=-0.0665$ MeV on the second sheet of the complex-energy Riemann surface, which implies a singlet effective range of 2.729 F. To fit this wave, we note that the antibound-state pole on the second or unphysical sheet leads to a zero in the S matrix at the corresponding position on the physical sheet of the complex-energy surface. The condition that the S matrix have a zero at $E_V=-0.0665$ MeV was used to obtain the attractive coupling strength. We then searched for the values of the repulsive coupling strength and the attractive and repulsive inverse ranges which give the best fit to the phase shift and the scattering length. Effective-range theory was then used to determine the value of the effective range produced by the separable-potential model. Our amplitudes are, therefore, *guaranteed* to contain the antibound state pole at the correct position on the unphysical sheet.

If we consider the partial wave $^3S_1$ as uncoupled, we demand that the S matrix have the deuteron pole at $E_D=-2.22452$ MeV on the physical sheet. This is obtained by forcing the denominator function D to have a zero at the pole position. This condition ($D=0$) was used to determine the attractive coupling strength. Then our search programs determined the values of the remaining three parameters which gave the best fit to the phase shift and scattering length. Later we obtained the effective range from Eq. (11).

When we at last consider the coupled waves $^3S_1$ and $^3D_1$, we again guarantee the correct binding energy for the deuteron by obtaining the attractive strength in $l=0$ from the condition that $D=0$ at $E_D=-2.22452$ MeV. Next we searched for the values of the remaining seven parameters which yielded the best fit to the phase shifts, mixing parameter, scattering length, deuteron quadrupole moment, and D-state probability. The effective range was obtained as before, from Eq. (11). Since the quadrupole moment of the deuteron depends on the off-energy-shell behavior of the two-nucleon interaction, we weighted this quantity so that our searching routines were heavily biased in favor of those parameter sets that led to a nearly correct quadrupole moment. We found that the resulting D-state probabilities were quite low. However, since the available estimates of the D-state probability are imprecise and seem to be somewhat model-dependent, we do not believe that these low D-state probabilities constitute a serious drawback. Table X gives the low-energy parameters resulting from our fits.

For the coupled waves $J=2$ and $J=4$, we were able to reproduce the phase shifts and mixing parameters with four parameters, an attractive strength and inverse range in $J+1$ and an attractive strength and inverse range in $J-1$. In the coupled waves $J=3$, we need six parameters to fit the phase shifts and mixing parameters. Since there is no attractive force for $J+1$, our separable-potential formalism guarantees that the mixing parameter is positive. Note that if we had taken only the repulsion needed to reproduce $^3G_3$ and the attraction

TABLE VII. Case-I fits to nucleon-nucleon phase shifts in coupled waves, assuming $\epsilon_J=0$ and neglecting δ_{J+1}. These partial waves are fitted by the separable potential

$$V_l(p,p')=g_l(p)g_l(p')-h_l(p)h_l(p'),$$

where the form factors are

$$g_l(p)=C_R p^l/(p^2+a_R^2)^{(l+1)/2},\quad h_l(p)=C_A p^l/(p^2+a_A^2)^{(l+1)/2},$$

except in the SR fits to the partial wave $^3S_1$, where the repulsive form factor is

$$g_l^R(p)=C_R p^{l+2}/(p^2+a_R^2)^{(l+3)/2}.$$

The units of the attractive inverse range a_A and the repulsive inverse range a_R are inverse fermis (F^{-1}, 1 F$=10^{-13}$ cm). The units of the attractive coupling strength C_A and the repulsive coupling strength C_R are (MeV F)$^{1/2}$. Dots indicate that a form factor is to be set equal to zero. $\sum R^2$ is the sum of the squares of the residuals,

$$\sum R^2=\sum_{i=1}^{50}[\delta_l^{\text{expt}}(E_i)-\delta_l^{\text{fit}}(E_i)]^2,$$

over the 50 data spaced at 8-MeV intervals in the range 0–400 MeV.

Partial wave	Repulsive potential parameters a_R (F^{-1})	C_R [(MeV F$^{1/2}$)]	Attractive potential parameters a_A (F^{-1})	C_A [(MeV F$^{1/2}$)]	ΣR^2
$^3S_1$	2.230	75.58	2.044	70.48	174.6
$^3S_1$ SR	2.036[a]	76.46[a]	1.735	12.45	179.8
$^3P_2$	···	···	1.406	5.007	4.933
$^3D_3$	···	···	1.836	4.647	0.0470
$^3F_4$	···	···	1.562	4.176	0.154

[a] Special repulsive form factor must be used.

TABLE VIII. Case-II fits to nucleon-nucleon phase shifts in coupled waves, assuming $\epsilon_J=0$ and neglecting δ_{J+1}. These partial waves are fitted by the separable potential

$$V_l(p,p')=g_l(p)g_l(p')-h_l(p)h_l(p'),$$

where the form factors are

$$g_l(p)=C_R p^l/(p^2+a_R^2)^{(l+2)/2},\quad h_l(p)=C_A p^l/(p^2+a_A^2)^{(l+2)/2},$$

except in the SR fits to the partial wave $^3S_1$, where the repulsive form factor is

$$g_l^R(p)=C_R p^{l+2}/(p^2+a_R^2)^{(l+4)/2}.$$

The units of the attractive inverse range a_A and the repulsive inverse range a_R are inverse fermis (F^{-1}, 1 F$=10^{-13}$ cm). The units of the attractive coupling strength C_A and the repulsive coupling strength C_R are (MeV F)$^{1/2}$. Dots indicate that a form factor is to be set equal to zero. $\sum R^2$ is the sum of the squares of the residuals,

$$\sum R^2\equiv\sum_{i=1}^{50}[\delta_l^{\text{expt}}(E_i)-\delta_l^{\text{fit}}(E_i)]^2,$$

over the 50 data spaced at 8-MeV intervals in the range 0–400 MeV.

Partial wave	Repulsive potential parameters a_R (F^{-1})	C_R [(MeV F$^{1/2}$)]	Attractive potential parameters a_A (F^{-1})	C_A [(MeV F$^{1/2}$)]	ΣR^2
$^3S_1$	2.624	84.69	2.176	68.10	164.9
$^3S_1$ SR	2.515[a]	62.67[a]	1.330	13.82	186.6
$^3P_2$	···	···	2.080	21.62	0.310
$^3D_3$	···	···	2.366	22.50	0.020
$^3F_4$	···	···	1.977	18.51	0.319

[a] Special repulsive form factor must be used.

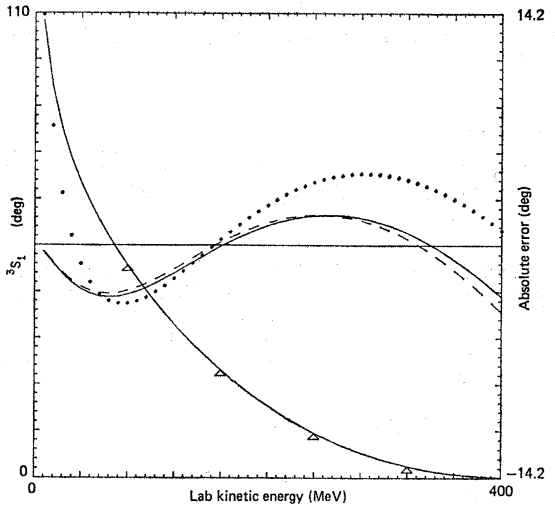

FIG. 26. Fits to the triplet phase shift $^3S_1$ (assuming $\epsilon_1=0$ and neglecting δ^3D_1). Description of curves is as for Fig. 1.

needed to fit $^3D_3$, this attempt at a four-parameter fit would have $\epsilon_3=0$.

We would like to point out that our fits to the important phase parameters $^1P_1$, $^3S_1$, and $^3D_1$ deviate from the energy-dependent data curves in the same way as the energy-independent data points of the Livermore phase-shift analysis.

Generally speaking, our type-II fits seem to be the most successful and this is particularly fortunate since all the relevant integrals can be done analytically for $l=0$ and $l=2$. The type-III fits are the least successful, except in the higher partial waves. We have not given values of χ^2 since this number is meaningless without some knowledge of the error in the input data, which is not available for the Livermore energy-dependent phase shifts.

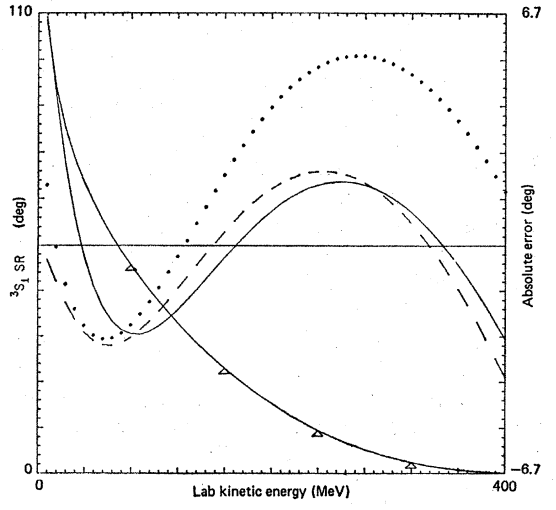

FIG. 27. SR fits to the triplet phase shift $^3S_1$ (assuming $\epsilon_1=0$ and neglecting δ^3D_1) with special repulsive form factor. Description of curves is as for Fig. 1.

TABLE IX. Case-III fits to nucleon-nucleon phase shifts in coupled waves, assuming $\epsilon_J=0$ and neglecting δ_{J+1}. These partial waves are fitted by the separable potential

$$V_l(p,p')=g_l(p)g_l(p')-h_l(p)h_l(p'),$$

where the form factors are

$$g_l(p)=G_R[(1/\pi p^2)Q_l(1+\mu_R^2/2p^2)]^{1/2},$$
$$h_l(p)=G_A[(1/\pi p^2)Q_l(1+\mu_A^2/2p^2)]^{1/2},$$

except in the SR fits to the partial wave $^3S_1$, where the repulsive form factor is

$$g_l^R(p)=[G_Rp^2/(p^2+\tfrac{1}{4}\mu_R^2)][(1/\pi p^2)Q_l(1+\mu_R^2/2p^2)]^{1/2}.$$

The units of the attractive inverse range μ_A and the repulsive inverse range μ_R are inverse fermis (F^{-1}, 1 F$=10^{-13}$ cm). The units of the attractive coupling strength G_A and the repulsive coupling strength G_R are (MeV F)$^{1/2}$. Dots indicate that a form factor is to be set equal to zero. $\sum R^2$ is the sum of the squares of the residuals,

$$\sum R^2\equiv\sum_{i=1}^{50}[\delta_l^{\text{expt}}(E_i)-\delta_l^{\text{fit}}(E_i)]^2,$$

over the 50 data spaced at 8-MeV intervals in the range 0–400 MeV.

Partial wave	Repulsive potential parameters μ_R (F^{-1})	G_R [(MeV F)$^{1/2}$]	Attractive potential parameters μ_A (F^{-1})	G_A [(MeV F)$^{1/2}$]	ΣR^2
$^3S_1$	4.326	300.0	1.818	39.52	690.8
$^3S_1$ SR	3.387[a]	200.0[a]	3.092	28.27	646.2
$^3P_2$	...	...	1.437	8.952	22.90
$^3D_3$	...	...	2.048	11.96	0.248
$^3F_4$	...	...	1.620	12.14	0.0158

[a] Special repulsive form factor must be used.

Once the best values of the separable-potential parameters were found, it seemed desirable to have an independent check on our work. Therefore, the separable potentials were put into computer programs that solve the Lippmann-Schwinger equations (1) and (2) as complex matrix-inversion problems. The latter programs were developed completely independently of the present work. Since the values of the T matrices and phase parameters calculated from the two approaches agree, this constitutes an independent check of our results.

V. USE OF FITS

These fits can be used in a straightforward manner to reproduce the on-shell scattering amplitude. The separable-potential approach also provides a convenient extension of the scattering amplitude off the energy shell.

For calculations involving off-energy-shell nucleon-nucleon scattering amplitudes, we suggest the following approach. In our separable-potential formalism,

$$T_{ll'}(p,p';k^2)=N_{ll'}(p,p';k^2)/D(k^2),$$

where $l=l'$ for uncoupled waves. Thus, when $T_{ll'}(k^2)\neq0$,

$$T_{ll'}(p,p';k^2)=F_{ll'}(p,p';k^2)T_{ll'}(k^2), \qquad (16)$$

where

$$F_{ll'}(p,p';k^2)=N_{ll'}(p,p';k^2)/N_{ll'}(k,k';k^2)$$

and

$$F_{ll'}(k,k';k^2)\equiv F_{ll'}(k^2)=1.$$

TABLE X. Low-energy parameters.[a]

$^1S_0$ parameters

	Singlet scattering length a_s (F)	Singlet effective range r_s (F)
Experiment	−23.678	2.729
Case-I fit	−23.679	2.728
Case-II fit	−23.677	2.731
Case-III fit	−23.681	2.722

$^3S_1$ parameters (coupling to $^3D_1$ neglected)

	Triplet scattering length a_t (F)	Triplet effecttive range r_t (F)
Experiment	5.396	1.726
Case-I fit	5.391	1.719
with SR	5.394	1.723
Case-II fit	5.393	1.722
with SR	5.567	1.938
Case-III fit	5.406	1.739
with SR	5.411	1.745

$J=1$ parameters

	Triplet scattering length a_t (F)	Triplet effective range r_t (F)	Deuteron quadrupole moment (F^{-2})	Deuteron D-state probability (%)
Experiment	5.396	1.726	0.278	···
Case-I fit	5.655	2.042	0.277	0.7
with SR	5.482	1.834	0.276	1.0
Case-II fit	5.394	1.723	0.278	1.1
with SR	5.592	1.968	0.278	0.8
Case-III fit	5.988	2.409	0.278	0.5
with SR	5.634	2.018	0.276	0.5

[a] All fits to the partial waves $^1S_0$ contain a singlet antibound-state pole at $E=-0.0665$ MeV on the second or unphysical sheet of the complex-energy Riemann surface. All fits to the $J=1$ coupled-wave system and to the $^3S_1$ partial wave neglecting the coupling to $^3D_1$ contain the deuteron pole at $E=-2.22452$ MeV on the physical sheet of the complex-energy Riemann surface.

Now, we can use Eq. (16) in calculations with $F_{ll'}(p,p';k^2)$ obtained from the separable-potential model and $T_{ll'}(k^2)$ expressed directly in terms of the experimental phase shifts and mixing parameters. Of course, the expression for $T_{ll'}(p,p';k^2)$ in Eq. (16) is still separable in the incident and outgoing momenta p and p'. Similarly, if $T_{ll'}(k_0^2)=0$ we have $N_{ll'}(k_0^2)=0$ and

$$T_{ll'}(p,p';k^2)=\frac{N_{ll'}(p,p';k^2)}{N_{ll'}{}^{(i)}(k_0^2)}T_{ll'}{}^{(i)}(k_0^2)$$

for $k^2\approx k_0^2$, where $N_{ll'}{}^{(i)}(k_0^2)$ and $T_{ll'}{}^{(i)}(k_0^2)$ are the first derivatives of $N_{ll'}(k^2)$ and $T_{ll'}(k^2)$ evaluated at $k^2=k_0^2$. Thus we have, for $k^2\approx k_0^2$,

$$T_{ll'}(p,p';k^2)=F_{ll'}{}^0(p,p';k^2)T_{ll'}{}^{(i)}(k_0^2), \quad (17)$$

where

$$F_{ll'}{}^0(p,p';k^2)=N_{ll'}(p,p';k^2)/N_{ll'}{}^{(i)}(k_0^2),$$

and again the off-shell amplitude is given by the product of a separable factor obtained from the separable-potential model and a quantity dependent only on the on-shell scattering data.

By using Eqs. (16) and (17), the exact experimentally determined scattering amplitude for $k^2>0$, in terms of the phase shifts and mixing parameters, can be inserted into calculations and the model dependence will lie only in the treatment of the region $k^2<0$ and of off-energy-shell effects. The desirability of this separation between on-shell and off-shell effects is indicated by recent p-p bremsstrahlung calculations.[13] In these calculations, the small differences between the on-shell predictions of various potentials seem to influence the results as much as the inclusion of off-energy-shell effects. With our approach any difference in the results of two potential models will be a consequence only of differences in off-energy-shell predictions. Although similar separations of on-shell and off-shell behavior can be made for local

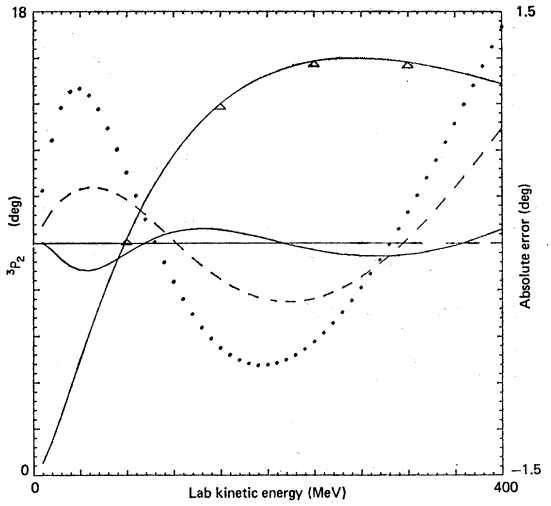

FIG. 28. Fits to the triplet phase shift $^3P_2$ (assuming $\epsilon_2=0$ and neglecting δ^3F_2). Description of curves is as for Fig. 1.

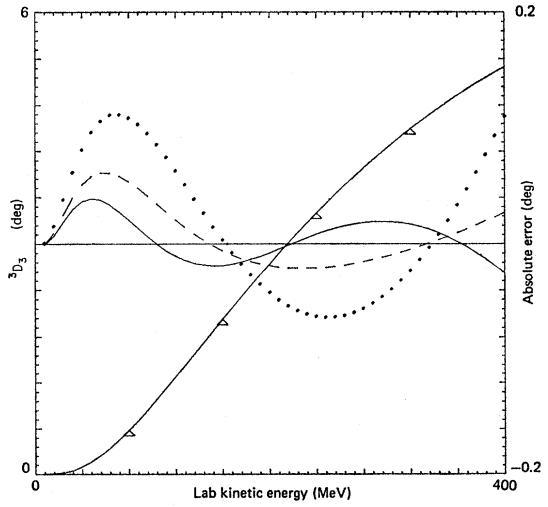

FIG. 29. Fits to the triplet phase shift $^3D_3$ (assuming $\epsilon_3=0$ and neglecting δ^3G_3). Description of curves is as for Fig. 1.

[13] W. A. Pearce, W. A. Gale, and I. M. Duck, Nucl. Phys. **B3**, 241 (1967).

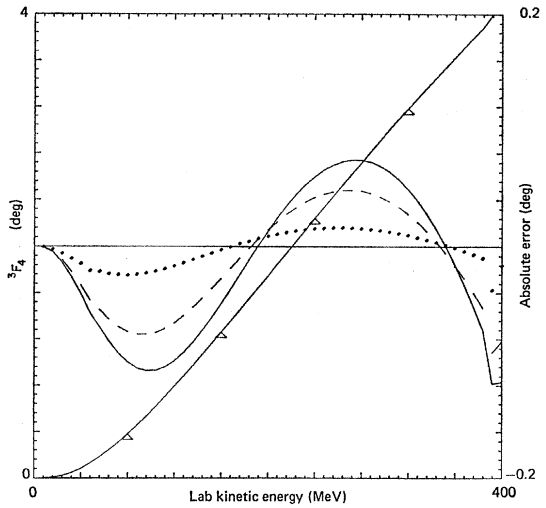

FIG. 30. Fits to the triplet phase shift $^3F_4$ (assuming $\epsilon_4=0$ and neglecting δ^3H_4). Description of curves is as for Fig. 1.

potentials,[1] they are *much* simpler and easier to use in a separable-potential formalism.

If we use several different models for the off-energy-shell scattering amplitude in a single calculation, we should get an indication of the dependence of the calculation on off-energy-shell behavior and $k^2<0$ behavior. This is particularly true in the approach that we have proposed, where we *know* that the on-shell amplitude for $k^2>0$ is represented exactly, and the only possible difference between the different calculations lies in $k^2<0$ or off-energy-shell effects. We might find that many calculations are relatively insensitive to the details of the off-energy-shell behavior of scattering amplitudes.

The fits that we have given will go immediately into any calculations involving nucleons that have been set up to use separable potentials and, in particular, they can be used directly in calculations based on the Tabakin potential. Some of the integrals involved in our fits will have to be done numerically and put into computing machines in tabular form, but this is a very simple matter.

ACKNOWLEDGMENTS

I would like to thank Dr. Joseph V. Lepore and Dr. Robert J. Riddell for their friendship, support, and encouragement. I am grateful to Dr. Richard A. Arndt and Dr. Malcom MacGregor for providing me with the phase-shift data in a convenient form prior to publication. I would especially like to thank Eric R. Beals, William F. Dempster, Dr. Loren P. Meissner, and Carl Quong of the Mathematics and Computing Group at the Lawrence Radiation Laboratory. Their assistance in the completion of this work was invaluable.